Electronic Supplementary Material (ESI) for Biomaterials Science.
This journal is © The Royal Society of Chemistry 2021

Supporting Information

Precise regulation of the properties of hydrophobic carbon dots by manipulating the structural feature of precursor ionic liquids

Tingting Guo, Xiaojuan Wang, Chenxi Zhao, Yang Shu*, Jianhua Wang*
Department of Chemistry, College of Sciences, Northeastern University, Shenyang, 110819, China.

*Corresponding author.

E-mail: shuyang@mail.neu.edu.cn, jianhuajrz@mail.neu.edu.cn.

Tel: +86 24 83688944

Supplementary Chemicals and Instrumentations

Supplementary Chemicals

Ethanol (EtOH), dimethylsulfoxide (DMSO), paraformaldehyde, sodium chloride (NaCl), potassium chloride (KCl), disodium phosphate (Na_2HPO_4), potassium dihydrogen phosphate (KH_2PO_4), hydrochloric acid (HCl) and sodium hydroxide (NaOH) were obtained from Sinopharm Chemical Reagent Co., Ltd. (Shanghai, China). The ionic liquids were purchased from Shanghai Cheng Jie Chemicals Co., Ltd. (Shanghai, China), including 1-ethyl-3-methylimidazolium dicyanamide (EmimDCN), 1-butyl-3-methylimidazolium dicyanamide (BmimDCN), 1-hexyl-3-methylimidazolium dicyanamide (HmimDCN), 1-octyl-3-methylimidazolium dicyanamide (OmimDCN), and 1-decyl-3-methylimidazolium dicyanamide (DmimDCN). Phenylbutazone and Ibuprofen were the products of Aladdin Bio-Chem Technology Co., Ltd. (Shanghai, China). Bovine serum albumin (BSA) were received from Sigma Aldrich (Shanghai, China). 3-(4,5-dimethylthiazol-2-yl)-2,5-diphenyltetrazolium bromide (MTT) assay kit was acquired from Nanjing KeyGEN Biotech (Nanjing, China). Dulbecco's modified medium (DMEM), fetal bovine serum, trypsin (25%) and penicillin/streptomycin were purchased from Thermo Scientific (Utah, USA). The reagents used were at least of analytical reagent grade. Deionized water of 18 MΩ/cm was employed throughout the experiments.

Supplementary Instrumentations

Transmission electron microscope (TEM) images were performed on JEM2100PLUS transmission electron microscope (JEOL, Japan). The water contact angle measurements were measured by using a DSA25 contact angle meter (KRÜSS, Germany). Fourier transform infrared (FT-IR) spectra were conducted on a VERTEX70 spectrophotometer (Bruker, Germany). X-ray photoelectron spectra (XPS) were acquired by using an ESCALAB 250 surface analysis system (Thermo Instruments Inc., USA). Elemental analysis data were recorded on Vario EL cube element analyzer (Elementar, Germany). Ultraviolet-visible (UV-vis) absorption

spectra were performed with a U-3900 UV-vis spectrophotometer (Hitachi High Technologies, Japan). F-7000 fluorescence spectrophotometer (Hitachi High Technologies, Japan) was used to record the fluorescence spectra. Quantaurus-QY absolute photoluminescence quantum yield measurement system (Hamamatsu Photonics, Japan) was exploited to obtain the quantum yield. Synergy H_1 Microplate reader (Biotek, USA) was employed to measure the fluorescence quenching spectra (excitation/emission wavelength, $\lambda_{ex}/\lambda_{em}$=280/340 nm) and absorbance at 490 nm for MTT assays. MOS-450 automatic recording spectropolarimeter (Bio-Logic, France) was used to obtain the circular dichroism spectra. The cell images were recorded by a FV-1200 confocal fluorescence microscope (Olympus, Japan).

Supplementary Figures

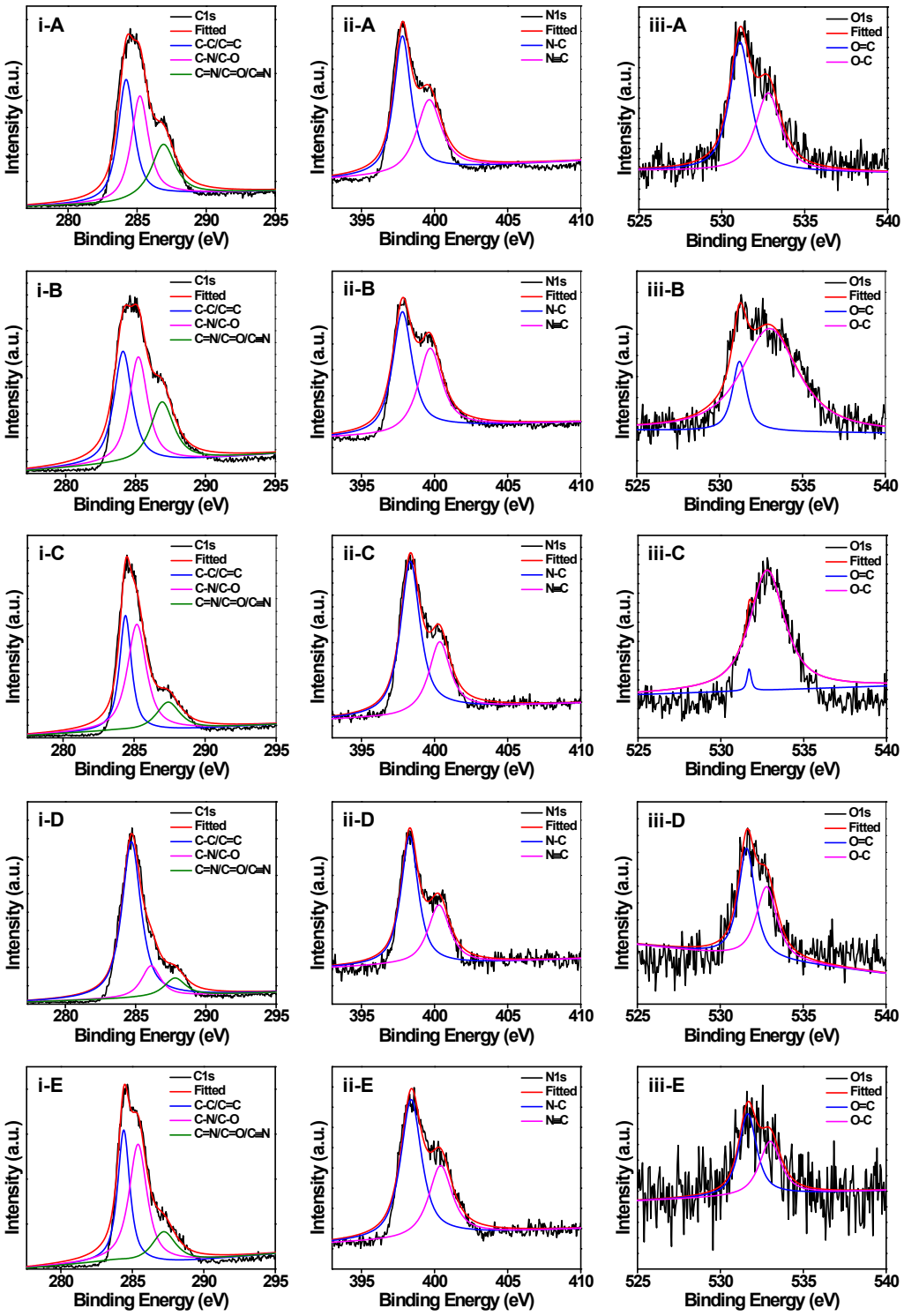

Fig. S1 The high resolution XPS spectra of C1s (i), N1s (ii) and O1s (iii) for the corresponding hydrophobic carbon dots (OCDs). (A) EOCDs, (B) BOCDs, (C) HOCDs, (D) OOCDs, and (E) DOCDs.

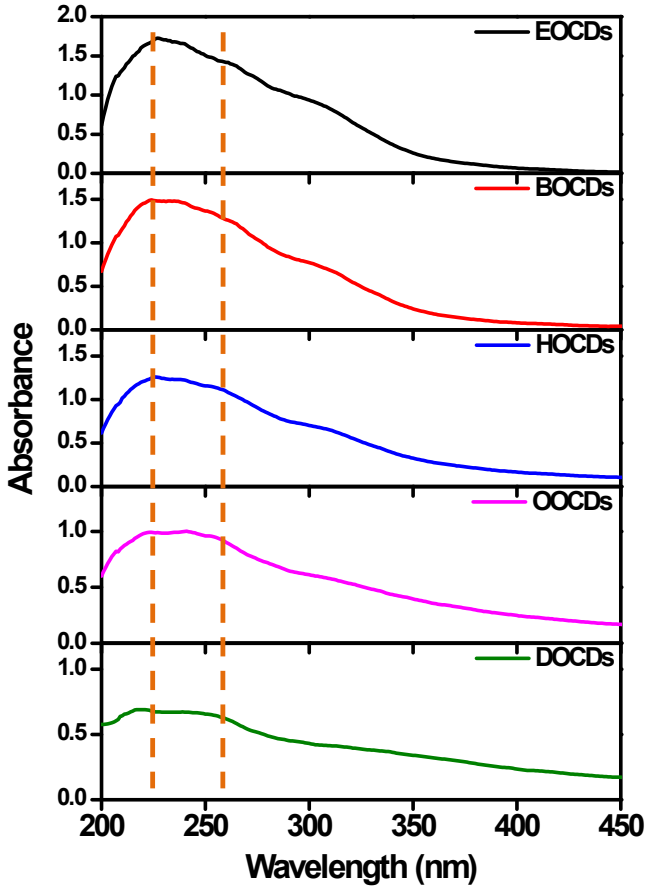

Fig. S2 UV-vis absorption spectra of the corresponding hydrophobic carbon dots (OCDs, 20 μg/mL). The solution contains 10% ethanol (V:V).

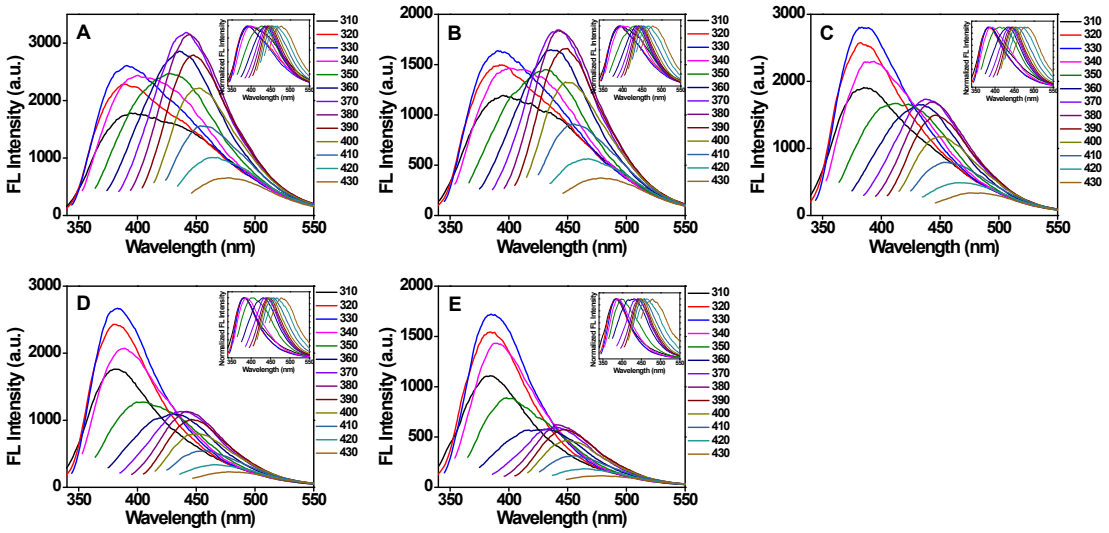

Fig. S3 Fluorescence emission spectra of the corresponding hydrophobic carbon dots (OCDs, 20 μg/mL). (A) EOCDs, (B) BOCDs, (C) HOCDs, (D) OOCDs, and (E) DOCDs. The insets are the normalized emission spectra. The solution contains 10% ethanol (V:V).

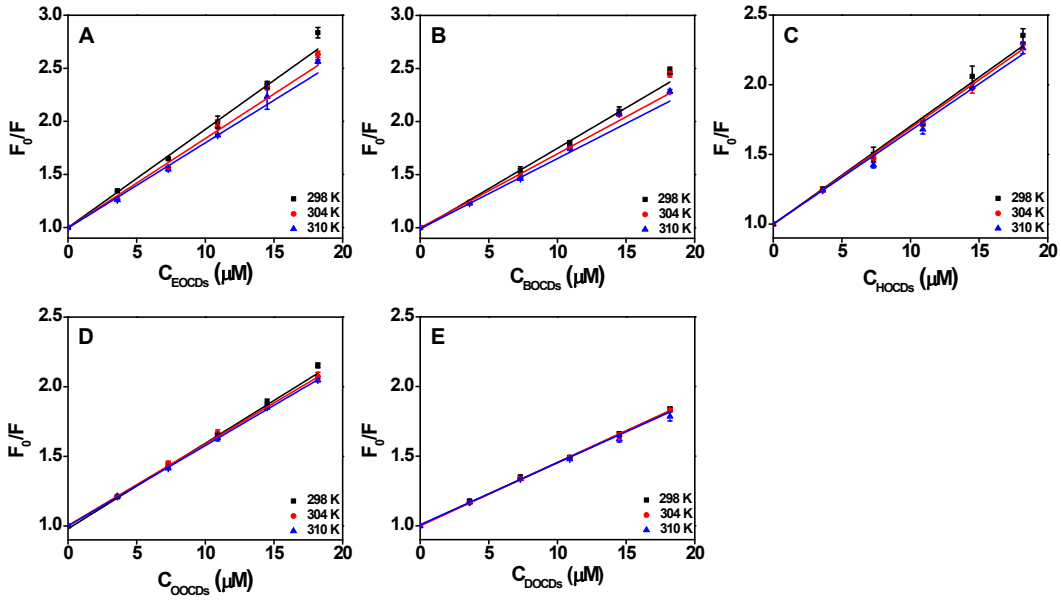

Fig. S4 The Stern-Volmer plot of fluorescence quenching of BSA induced by the corresponding hydrophobic carbon dots (OCDs) at different temperatures. (A) EOCDs, (B) BOCDs, (C) HOCDs, (D) OOCDs, (E) DOCDs. C_{BSA}=10 μM, pH 7.4. The solution contains 10% ethanol (V:V). The error bars indicate the standard deviations of three independent measurements.

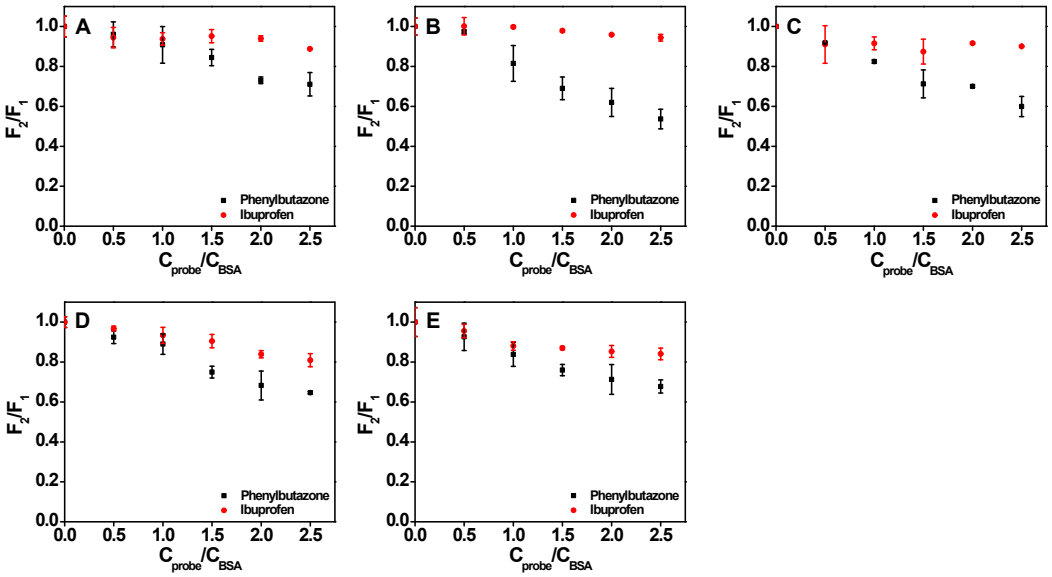

Fig. S5 The effect of site probes on the fluorescence of BSA in the interaction systems of (A) EOCDs/BSA, (B) BOCDs/BSA, (C) HOCDs/BSA, (D) OOCDs/BSA, (E) DOCDs/BSA, by the addition of different concentration of site probes. C_{OCDs}=20 μg/mL, C_{BSA}=10 μM. C_{probe}= 0, 5, 10, 15, 20, 25 μM. The solution contains 10% ethanol (V:V). The error bars indicate the standard deviations of three independent measurements.

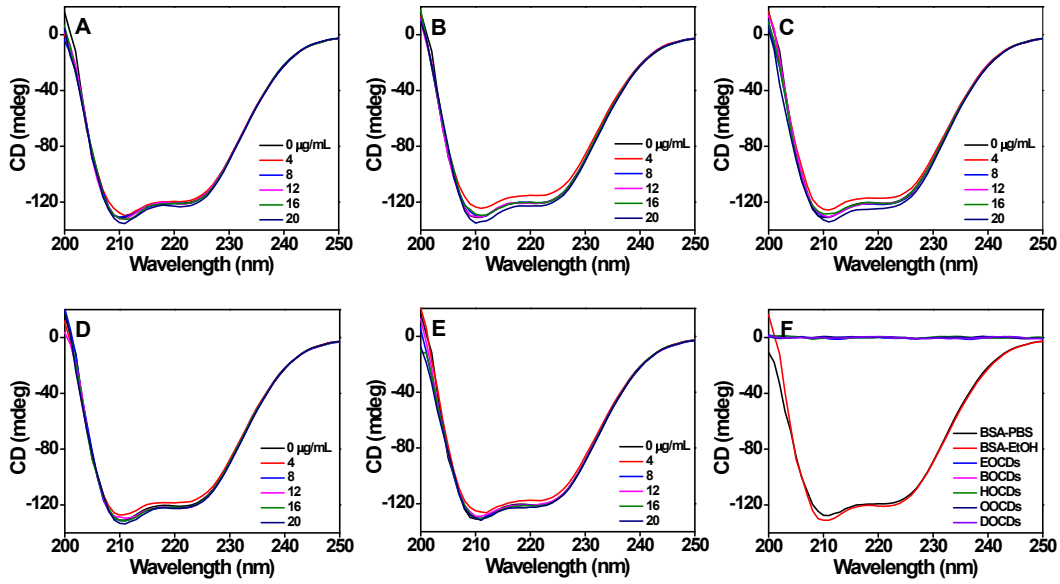

Fig. S6 The circular dichroism (CD) spectra of BSA after interaction with different concentrations of the corresponding hydrophobic carbon dots (OCDs). (A) EOCDs, (B) BOCDs, (C) HOCDs, (D) OOCDs, (E) DOCDs. (F) The CD spectra of the bare OCDs, in addition to the CD spectra of BSA in PBS (0.1 M) and ethanol (10%, V:V). C_{BSA}=10 μM, T=298 K, pH 7.4. The solution contains 10% ethanol (V:V).

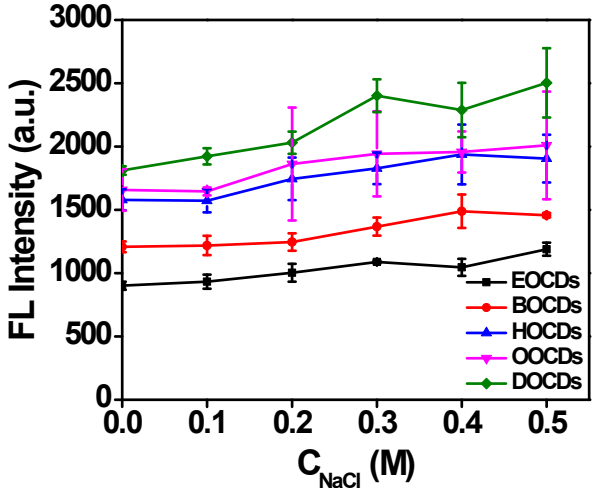

Fig. S7 The variation of fluorescence spectra of the OCDs/BSA interaction systems in the presence of various concentration of NaCl. The solution contains 10% ethanol (V:V). C_{OCDs}=20 μg/mL, C_{BSA}=10 μM. The error bars indicate the standard deviations of three independent measurements.

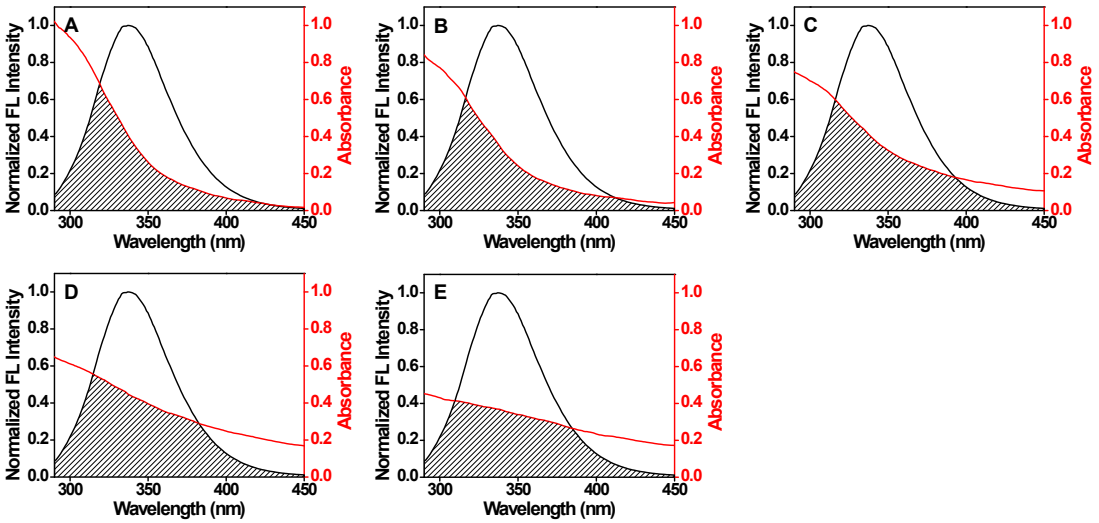

Fig. S8 The overlap of the fluorescence emission spectrum of BSA with the UV-vis absorption spectra of the corresponding hydrophobic carbon dots (OCDs). (A) EOCDs, (B) BOCDs, (C) HOCDs, (D) OOCDs, (E) DOCDs. C_{BSA}=10 μM, C_{OCDs}=20 μg/mL. The solution contains 10% ethanol (V:V).

Supplementary Results

The binding distance (r) between OCDs and BSA is evaluated by the theory of fluorescence resonance energy transfer (FRET). The efficiency of energy transfer between OCDs and Trp residues (E) may be calculated with the following equation, [1] with E as the efficiency of energy transfer between OCDs and BSA. r as the binding distance, and R_0 as the critical energy transfer distance when the efficiency is at 50%.

$$E = 1 - \frac{F}{F_0} = \frac{R_0^6}{R_0^6 + r_0^6} \qquad (1)$$

R_0 is derived by the following equation,

$$R_0^6 = 8.79 \times 10^{-25} K^2 N^{-4} \varphi J \qquad (2)$$

K^2 represents the spatial orientation factor related to the geometry of BSA and OCDs of dipoles, and K^2=2/3 for random orientation in fluid solution. N is the refracted

index of the medium. φ is QY for BSA and *J* is the spectral overlap between the fluorescence spectrum of BSA and absorption spectrum of OCDs. *J* is determined according to the following equation, with *F(λ)* and *ε(λ)* as fluorescence intensity of BSA and the molar absorption coefficient of OCDs within 290-450 nm.

$$J = \frac{\int_0^\infty F(\lambda)\varepsilon(\lambda)\lambda^4 d\lambda}{\int_0^\infty F(\lambda)d\lambda} \qquad (3)$$

In the present case, φ=0.49 and N=1.36, [2] and the values for *J*, E, R_0 and r are summarized in Table S4.

Supplementary References

1. Y.Z. Zhang, B. Zhou, X.P. Zhang, P. Huang, C.H. Li, Y. Liu, Interaction of malachite green with bovine serum albumin: determination of the binding mechanism and binding site by spectroscopic methods, *J. Hazard. Mater.* 163 (2009) 1345-1352.
2. T.T. Guo, A.Q. Zheng, X.W. Chen, Y. Shu, J.H. Wang, The structure-activity relationship of hydrophilic carbon dots regulated by the nature of precursor ionic liquids, J. Colloid Interface Sci. 554 (2019) 722–730.

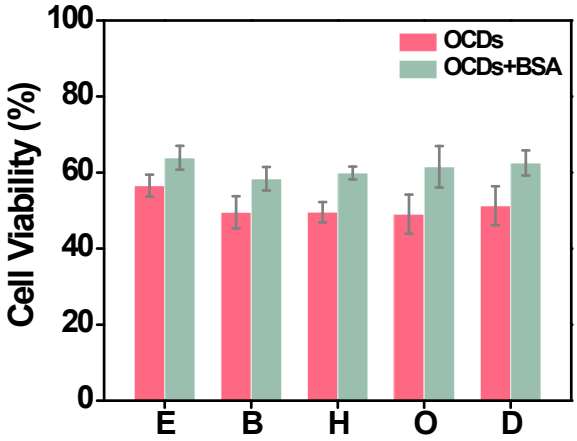

Fig. S9 The viabilities of MCF-7 cells after incubation with OCDs of IC_{50} concentration in the presence and absence of BSA (10 μM). The error bars indicate the standard deviations from three independent measurements.

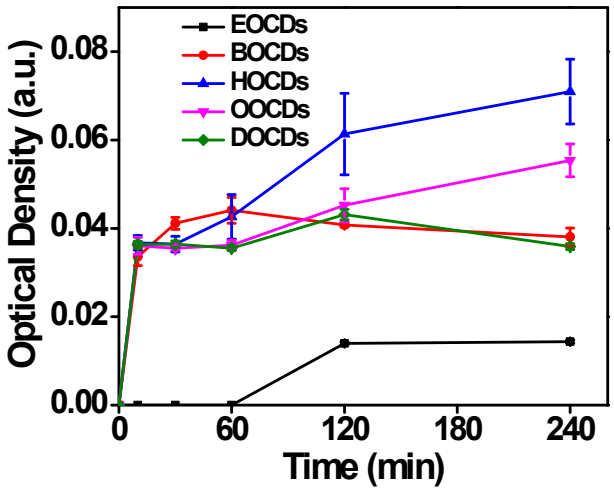

Fig. S10 Optical density of confocal fluorescence images treated with OCDs according to ImageJ software. The error bars indicate the standard deviations from three independent measurements.

Supplementary Table

Table S1 The structure of ILs (1-alkyl-3-methylimidazolium dicyanamide), the abbreviation of the corresponding product OCDs, zeta potential (2 mg/mL in ethanol) and elemental composition based on XPS analysis.

ILs' Name	ILs' Structure	Product abbreviation	Zeta potential (mV)	Elemental composition (%)		
				C	N	O
EmimDCN	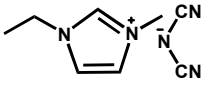	EOCDs	-13.57 ± 1.40	63.73	31.84	4.44
BmimDCN	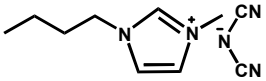	BOCDs	-5.69 ± 0.52	67.55	26.23	6.22
HmimDCN	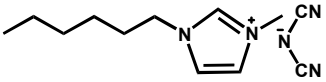	HOCDs	-7.39 ± 1.03	71.67	21.93	6.40
OmimDCN	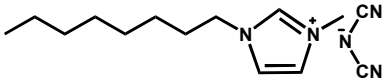	OOCDs	-7.12 ± 1.30	72.72	23.26	4.02
DmimDCN	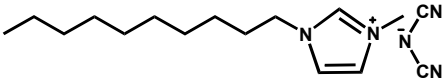	DOCDs	-12.03 ± 0.93	73.72	23.76	2.52

Table S2 The Stern-Volmer quenching constants K_{SV} and bimolecular quenching constants K_q for the OCDs/BSA interaction systems.

	Temp. (K)	K_{SV} ($\times 10^4$L/mol)	K_q ($\times 10^{12}$L/mol·s)	R^2
EOCDs	298	9.240	9.240	0.9958
	304	8.400		0.9924
	310	8.021		0.9952
BOCDs	298	7.614	7.614	0.9915
	304	6.967		0.9994
	310	6.610		0.9902
HOCDs	298	7.035	7.035	0.9968
	304	6.914		0.9978
	310	6.707		0.9982
OOCDs	298	6.139	6.139	0.9967
	304	5.868		0.9998
	310	5.777		0.9996
DOCDs	298	4.511	4.511	0.9986
	304	4.554		0.9995
	310	4.452		0.9978

R^2 is the correlation coefficient.

Table S3 The binding constants K_a, the average number of binding sites n and thermodynamic parameters (ΔH, ΔS and ΔG) for the OCDs/BSA interaction systems.

	T (K)	K_a ($\times 10^4$ L/mol)	n	R^2	ΔH (kJ/mol)	ΔS (kJ/mol·K)	ΔG (kJ/mol)
EOCDs	298	12.30	1.024	0.9928	59.89	0.3015	-29.96
	304	60.26	1.171	0.9980			-31.77
	310	30.90	1.118	0.9997			-33.58
BOCDs	298	36.31	1.138	0.9986	25.49	0.1934	-32.14
	304	74.13	1.207	0.9947			-33.30
	310	53.70	1.179	0.9966			-34.46
HOCDs	298	15.85	1.072	0.9933	-47.84	-0.05844	-30.42
	304	27.54	1.125	0.9969			-30.07
	310	7.413	1.009	0.9974			-29.72
OOCDs	298	13.49	1.070	0.9995	-50.58	-0.07308	-28.80
	304	5.129	0.9877	0.9991			-28.36
	310	6.166	1.006	0.9995			-27.92
DOCDs	298	4.266	0.9952	0.9951	-40.77	-0.04661	-26.88
	304	5.495	1.017	0.9990			-26.60
	310	2.239	0.9407	0.9973			-26.32

R^2 is the correlation coefficient.

Table S4 The spectral overlap *J*, the efficiency of energy transfer E, the critical energy transfer distance R_0 and the binding distance r for the OCDs/BSA interaction systems.

	J (10^{-14} (cm^2 L)/mol)	E (%)	R_0 (nm)	r (nm)
EOCDs-BSA	32.4	71	5.5	4.7
BOCDs-BSA	30.7	63	5.4	5.0
HOCDs-BSA	36.8	59	5.6	5.3
OOCDs-BSA	40.5	55	5.7	5.5
DOCDs-BSA	35.6	46	5.6	5.7